Science Advances
AAAS

Supplementary Materials for

Control of trion-to-exciton conversion in monolayer WS_2 by orbital angular momentum of light

Rahul Kesarwani, Kristan Bryan Simbulan, Teng-De Huang, Yu-Fan Chiang, Nai-Chang Yeh*, Yann-Wen Lan*, Ting-Hua Lu*

*Corresponding author. Email: ncyeh@caltech.edu (N.-C.Y.); ywlan@ntnu.edu.tw (Y.-W.L.); thlu@ntnu.edu.tw (T.-H.L.)

Published 1 April 2022, *Sci. Adv.* **8**, eabm0100 (2022)
DOI: 10.1126/sciadv.abm0100

This PDF file includes:

1. Surface morphology and Spectroscopic characterization of WS_2.

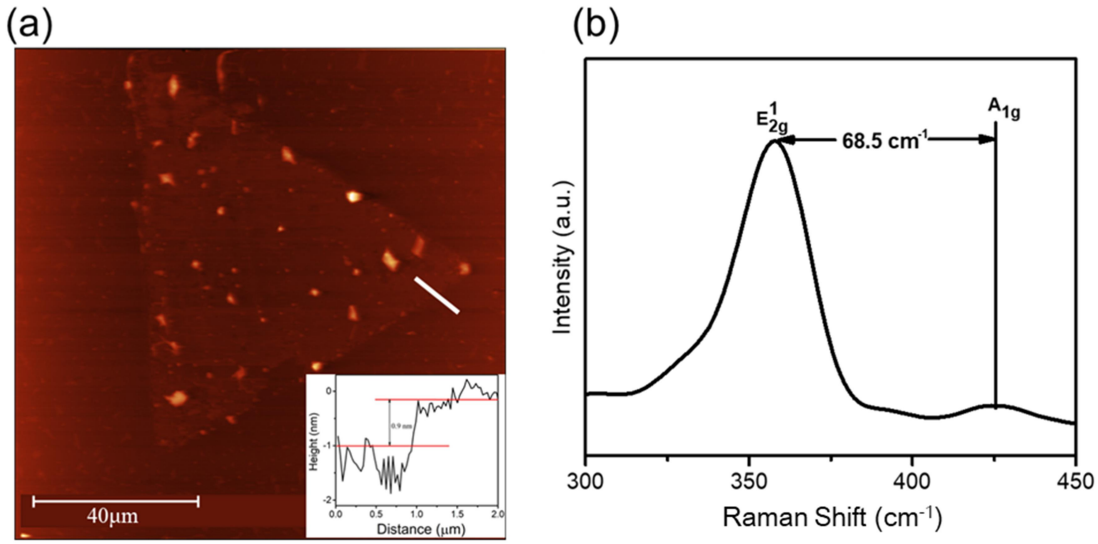

Figure S1. AFM image of single-layer WS_2 flake. Monolayer deposition of a CVD-grown WS_2 flake onto SiO_2/Si substrate confirmed by its (a) AFM image and (b) Raman spectrum.

2. Deconvolution of the exciton, trion and defects peaks in photoluminescence (PL) spectra excited by different orbital angular momentum (OAM) light at 300 K.

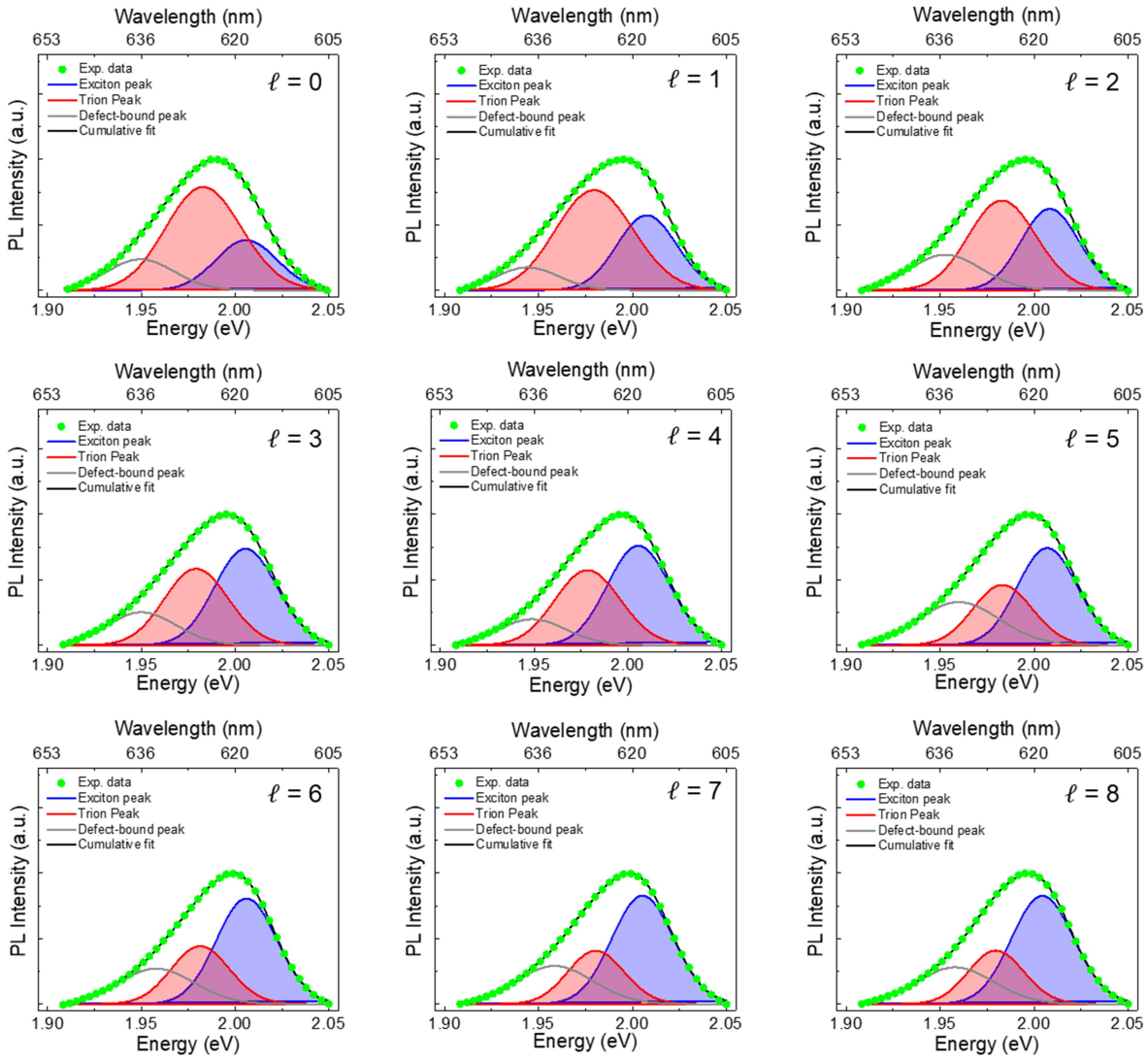

Figure S2. OAM light dependence of PL spectra at room temperature (RT). Deconvoluted RT (300 K) PL spectra of monolayer WS_2 excited by different value of OAM (ℓ) at 30 μW laser power. Each PL spectrum has been fitted by the superposition of three components as indicated by the blue, red, and gray curves, which correspond to the exciton, trion, and defect states, respectively. It is evident that the exciton intensity increases with the OAM value ℓ while the

trion intensity decreases. Similar procedure has been taken to analyze the PL spectra obtained by using other laser powers. These PL spectral analyses are used to estimate the trion-to-exciton conversion efficiency for a given OAM value by considering the trion-to-exciton intensity ratio.

3. Deconvolution of the exciton, trion and defects peaks in PL spectra excited by different OAM light at 77 K.

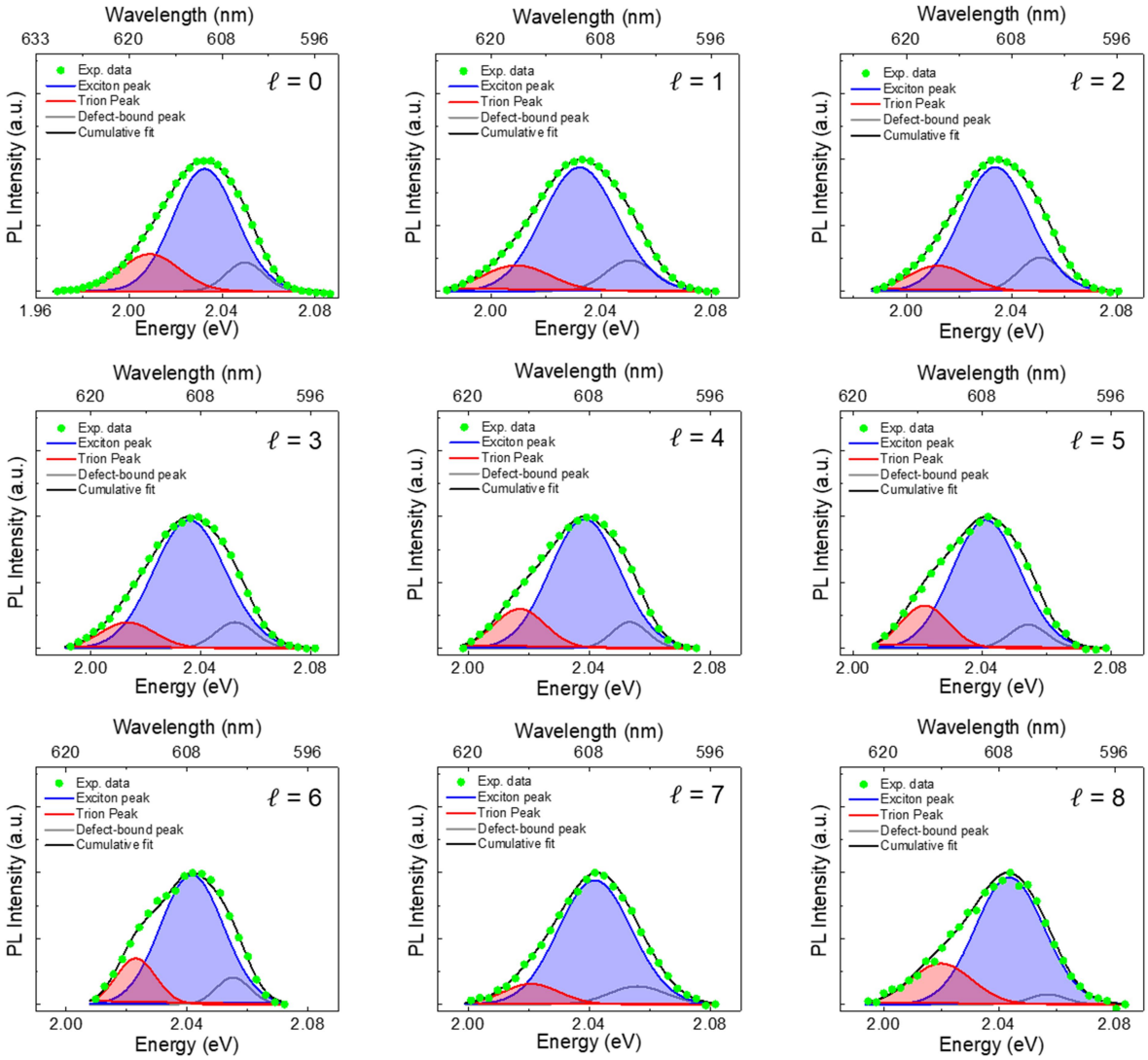

Figure S3. OAM light dependence of PL at 77 K. Deconvolution of the low temperature (77 K) PL spectra of monolayer WS_2 excited by different values of OAM at 30 μW laser power. Each PL spectrum has been fitted by the superposition of three components as indicated by the blue, red, and gray curves, which correspond to the exciton, trion, and defect states, respectively. It is

found that the trion-to-exciton intensity ratio is independent of the topological charge of the OAM light.

4. Fitting details of deconvoluted PL spectra taken at 300 K.

We used an origin software for fitting the PL spectra. The wavelengths for each peak are fixed within reasonable range from ~600 nm to ~650 nm (2.067 to 1.908 eV). For example, the fitting Adj. R-square value of PL spectra at 30 μW laser power for all values of ℓ are listed in Table S1. The full-width half maximum (FWHM) fitting error is listed which has been obtained after the deconvolution of PL spectra. However, the error bar putting in the reported figures is estimated via taking the average of repeating the PL measurements three times (each time deconvoluted the PL spectra).

Table S1. Coefficient of determination and fitting error at 300 K. Fitting parameters for the PL spectra of 30 μW laser power under different OAM values ℓ of light at 300 K.

OAM value, ℓ @30μW	Adj. R-square	Exciton FWHM fitting error (nm)	Trion FWHM fitting error (nm)
0	0.99977	0.216	1.390
1	0.99975	0.957	3.734
2	0.99969	0.051	0.762
3	0.99975	0.053	0.497
4	0.99967	0.059	0.663
5	0.99979	0.045	0.407
6	0.99974	0.045	0.459
7	0.99976	0.038	0.408
8	0.9998	0.035	0.359

5. Fitting details of deconvoluted PL spectra taken at 77 K.

We used an origin software for fitting the PL spectra. The wavelengths for each peak are fixed within reasonable range from ~600 nm to ~630 nm (2.067 to 1.968 eV). For example, the fitting Adj. R-square value of PL spectra at 30 μW laser power for all values of ℓ are listed in Table S1. The FWHM fitting error is listed which has been obtained after the deconvolution of PL spectra.

Table S2. Coefficient of determination and fitting error at 77 K. Fitting parameters for the PL spectra of 30 μW laser power under different OAM values ℓ of light at 77 K.

OAM value, ℓ @30μW	Adj. R-square	Exciton FWHM fitting error (nm)	Trion FWHM fitting error (nm)
0	0.99983	0.107	0.105
1	0.99963	0.193	0.176
2	0.99947	0.243	0.199
3	0.9986	0.285	0.207
4	0.99771	0.267	0.157
5	0.998	0.292	0.126
6	0.99536	0.455	0.160
7	0.99864	0.486	0.284
8	0.99407	0.299	0.267

6. Comparison of the trion/exciton intensity ratio at fixed value of OAM light.

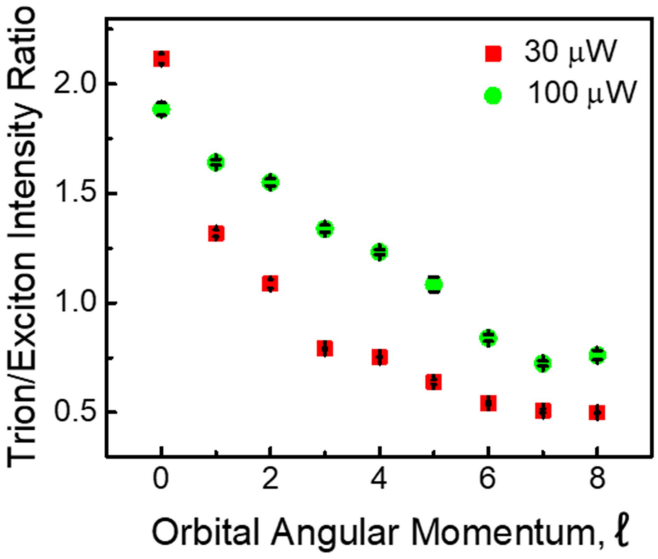

Figure S4. Intensity ratio between trion and exciton as function of OAM light at a fixed laser power. Comparison of the trion/exciton intensity ratio of monolayer WS_2 *vs.* the OAM value ℓ at 300 K under constant laser powers of 30 μW and 100 μW. It is found that the trion/exciton intensity ratio increases with increasing laser power for a given ℓ. These results suggest that the OAM of light can effectively suppress the trion/exciton emission, and a lower laser power leads to a higher conversion efficiency.

7. PL spectra for different topological charges of OAM and laser powers at 300 K.

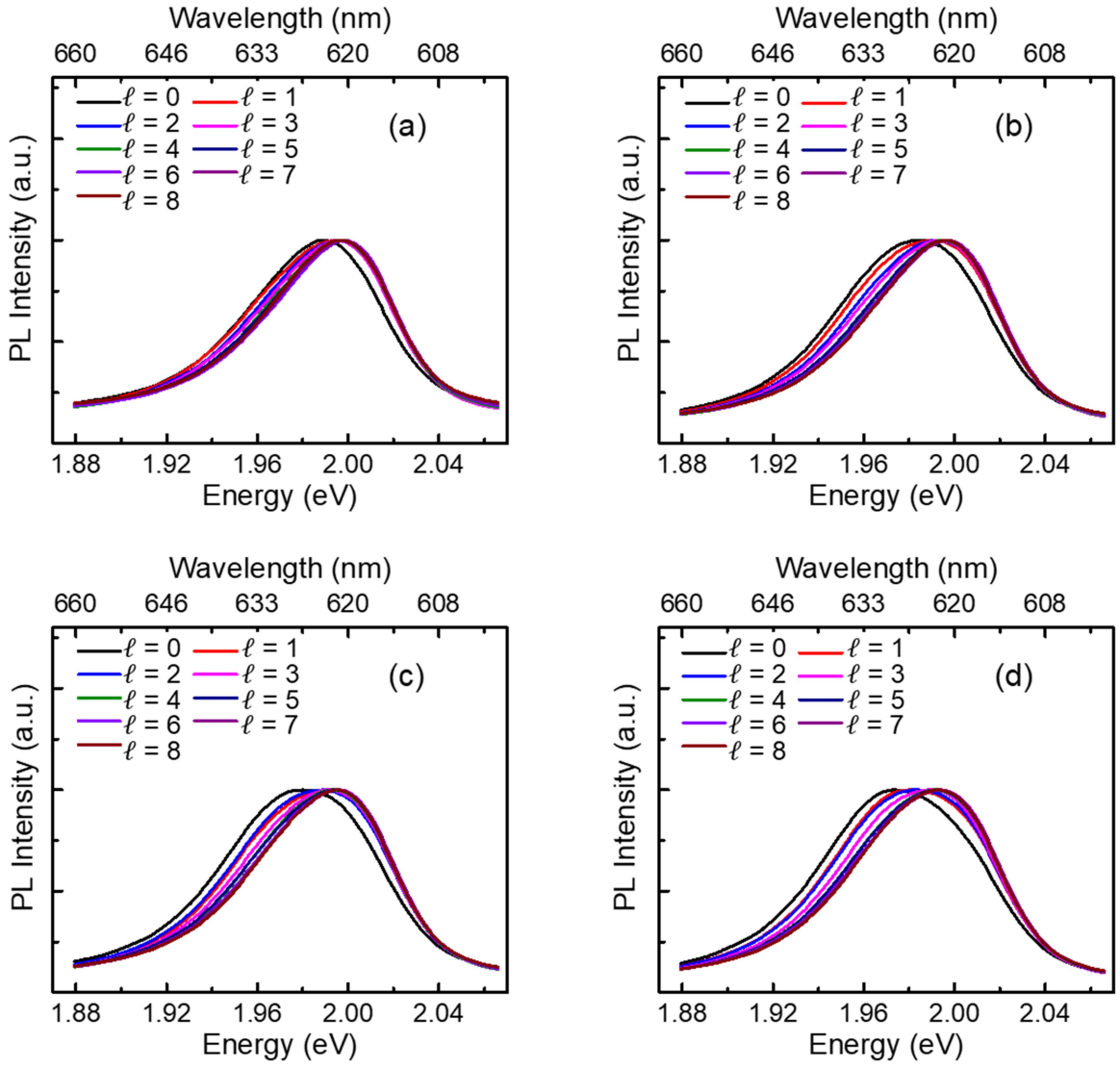

Figure S5. Power and OAM light dependence of PL spectra at 300 K. PL spectra of monolayer WS_2 at RT (300 K) measured via the modified in-house PL setup with different OAM of light (ℓ= 0 to 8) and laser powers: (a) 30 μW, (b) 50 μW, (c) 70 μW, and (d) 100 μW.

8. PL spectra for different topological charges of OAM and laser powers at 77 K.

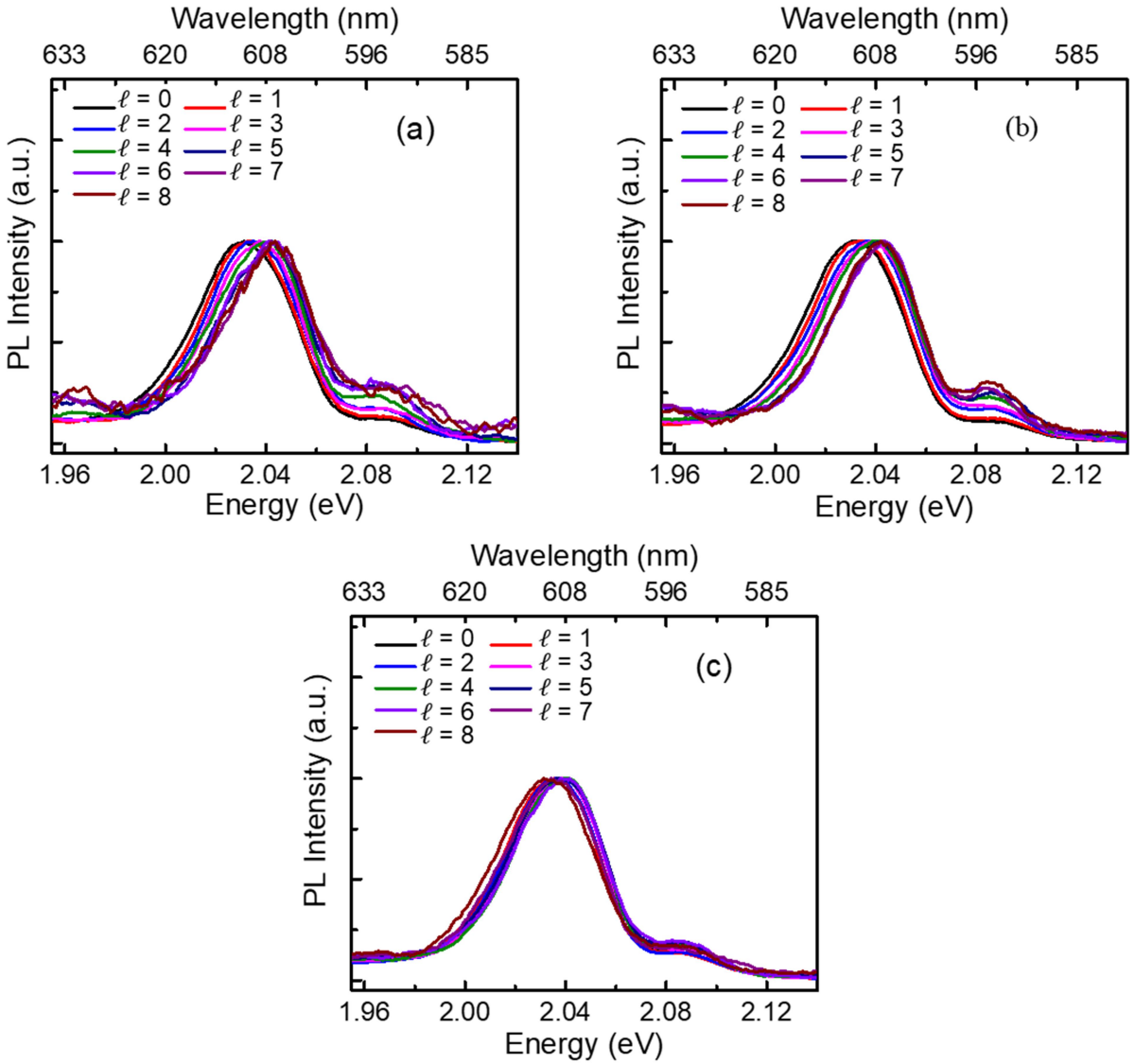

Figure S6. Power and OAM light dependence of PL spectra at 77 K. PL spectra of monolayer WS_2 at low temperature (77 K) in vacuum using the same PL setup with different OAM of light and laser powers: (a) 30 μW, (b) 50 μW, and (c) 100 μW. The PL spectra of monolayer WS_2 at 77 K exhibit showing an exciton-rich behavior for all values of OAM and laser powers. Notably, the intensity ratio at low temperature (77 K) is nearly independent of OAM.

9. Dependence of the peak position and intensity ratio of excitons and trions on the OAM at 300 K for laser powers ≤ 100 μW.

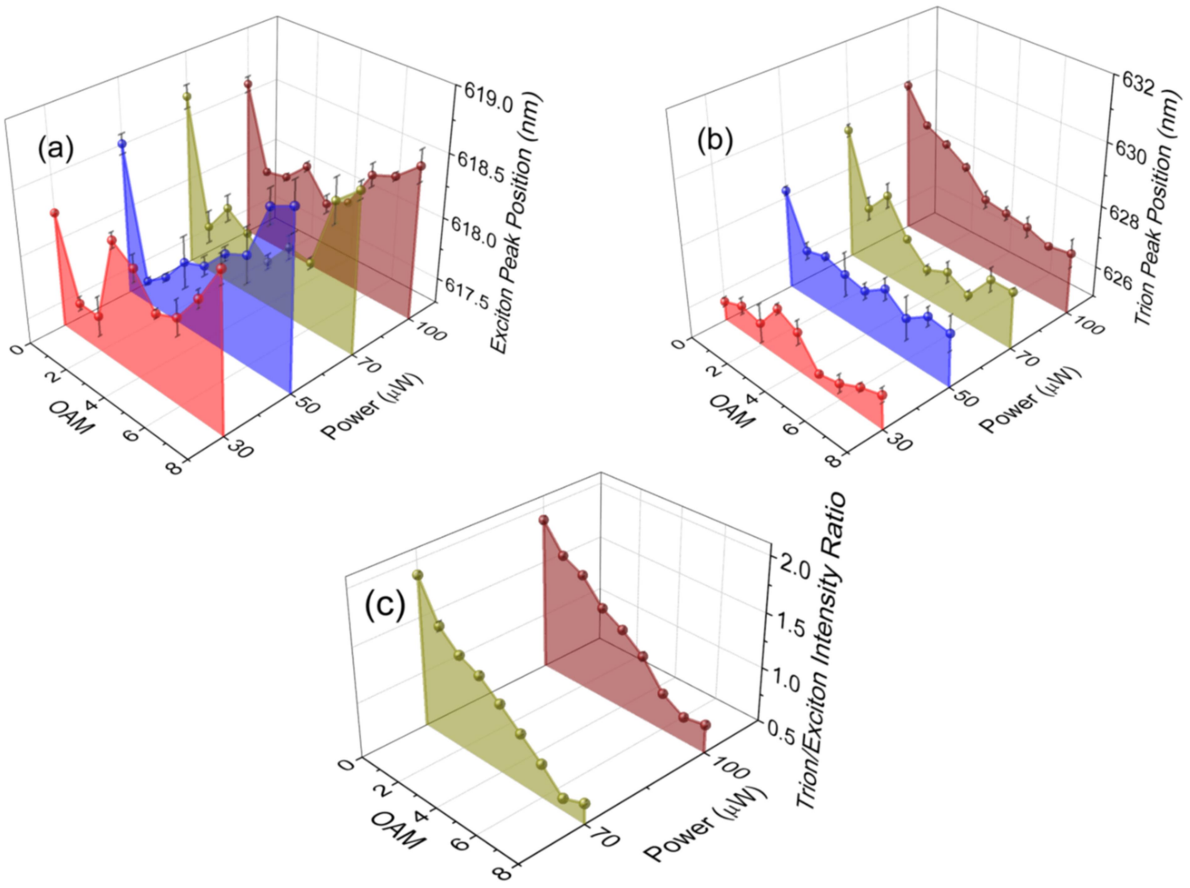

Figure S7. Data analysis of trion and exciton from PL spectra at 300 K. (a) and (b) are the PL peak positions of excitons and trions, respectively, of the monolayer WS_2 taken at 300 K for laser powers of 30 μW, 50 μW, 70 μW and 100 μW. (c) Variation of trion-to-exciton intensity ratio extracted from the monolayer WS_2 PL spectra at different OAM of light, which signifies that the conversion efficiency from trion-to-exciton is nearly the same for all laser powers.

10. Dependence of the peak position and intensity ratio of excitons and trions on the OAM at 77 K for laser powers ≤ 100 μW.

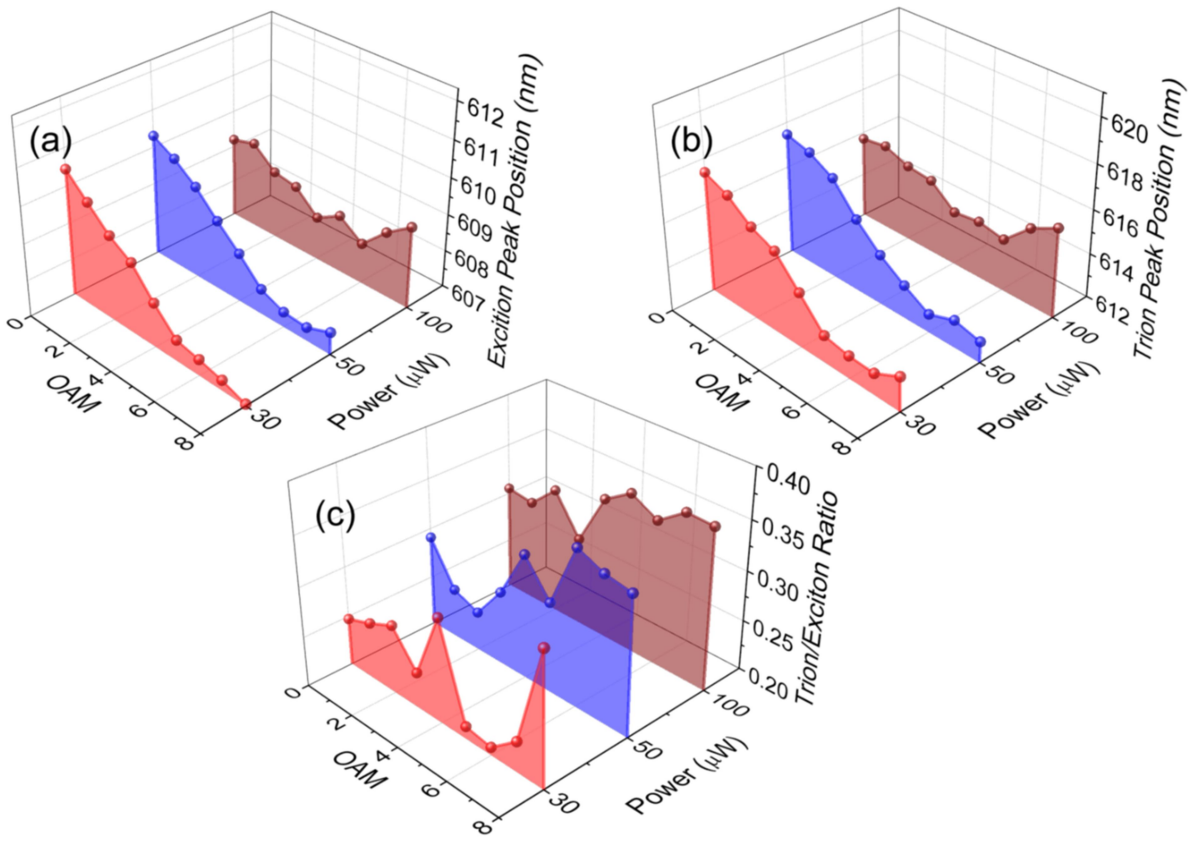

Figure S8. Data analysis of trion and exciton from PL spectra at 77 K. PL peak positions of (a) excitons and (b) trions, respectively, of the monolayer WS_2 at 77 K for 30 μW, 50 μW and 100 μW. (c) Variation of trion to exciton intensity ratio extracted from the monolayer WS_2 PL spectra at different OAM of light. The blue shifts in exciton and trion peaks around 3 - 4 nm (for 30 μW and 50 μW) have been observed when increasing the topological charge of OAM light from 0 to 8. We further note that the small and nearly constant trion-to-exciton intensity ratio with increasing OAM and laser power, signifies that the PL spectra monolayer WS_2 at 77 K are exciton-rich and independent of OAM.

11. Deconvolution of the exciton, trion and defects peaks in PL spectra under different gate voltages excited by odd values of OAM light for 100 μW laser power at 300 K.

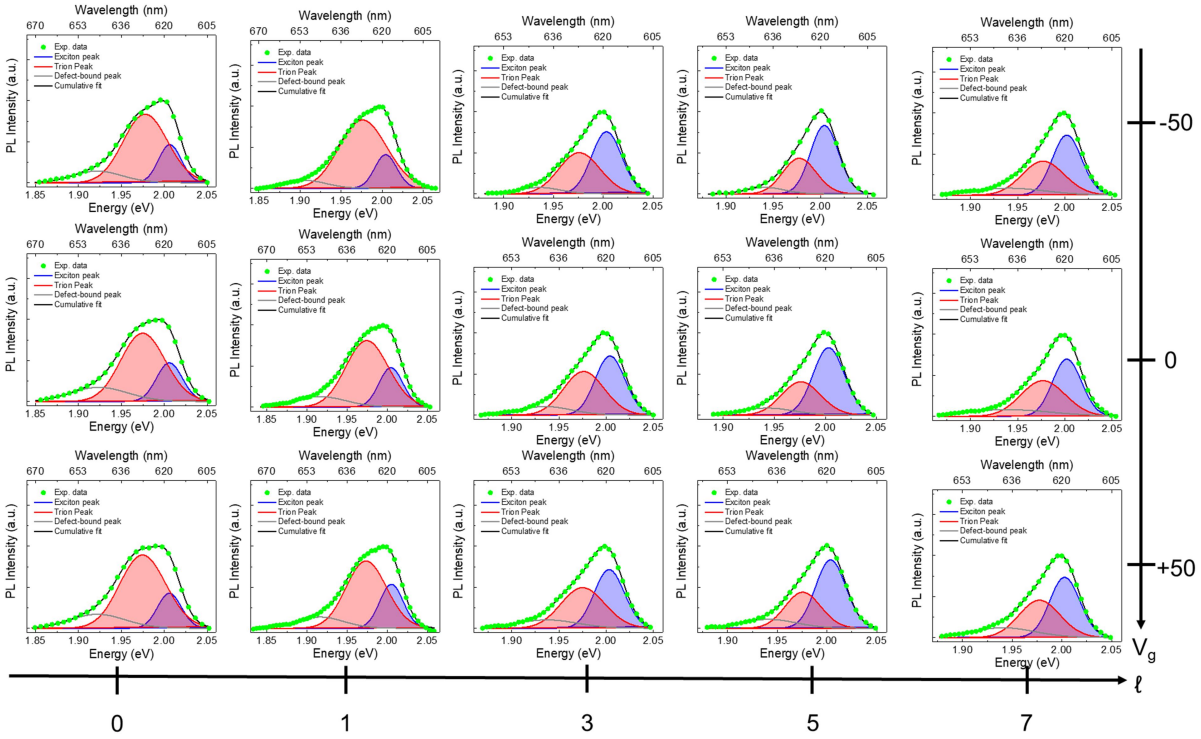

Figure S9. Gate voltage and OAM light dependence of deconvoluted PL spectra at 300 K. Deconvoluted PL spectra as a function of energy/wavelength of a monolayer WS_2 for an odd number of topological charges of OAM light (x-axis) under the excitation of 100 μW laser power at the gate voltage V_g of -50 V (top row), 0 V (middle row) and +50 V (bottom row) respectively. Each PL spectrum has been fitted by the superposition of three components as indicated by the blue, red, and gray curves, which correspond to the exciton, trion, and defect states, respectively. It found that the trion-to-exciton conversion with the topological charge of the OAM light is higher for positive gate voltage compare to that for negative voltage.

12. Effect of gate voltage on the intensity ratio and the conversion efficiency excited by odd values of OAM light for 100 μW laser power at 300 K.

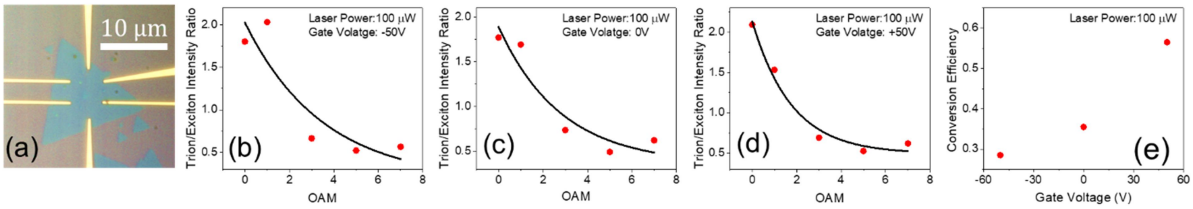

Figure S10. Gating effect on trion/exciton intensity ratio as function of OAM light. (a) Optical microscopy image of monolayer WS_2 flake on SiO_2/Si substrate with electrodes. Variations of the trion/exciton intensity ratio with the OAM value ℓ under a constant laser power of 100 μW at the gate voltage V_g of (b) -50 V, (c) 0 V, and (d) +50 V. (e) Trion-to-exciton conversion efficiency at 300 K as a function of gate voltage at a constant laser power of 100 μW. The trion-to-exciton conversion efficiency is smaller for a negative gate voltage (-50 V) and becomes larger for a positive gate voltage (+50 V). It is because positive gate voltage can induce more electrons to form trions, which is in contrast to the case of negative gate voltage for n-type semiconductor.

13. FWHM of trions and excitons at low temperature (77 K).

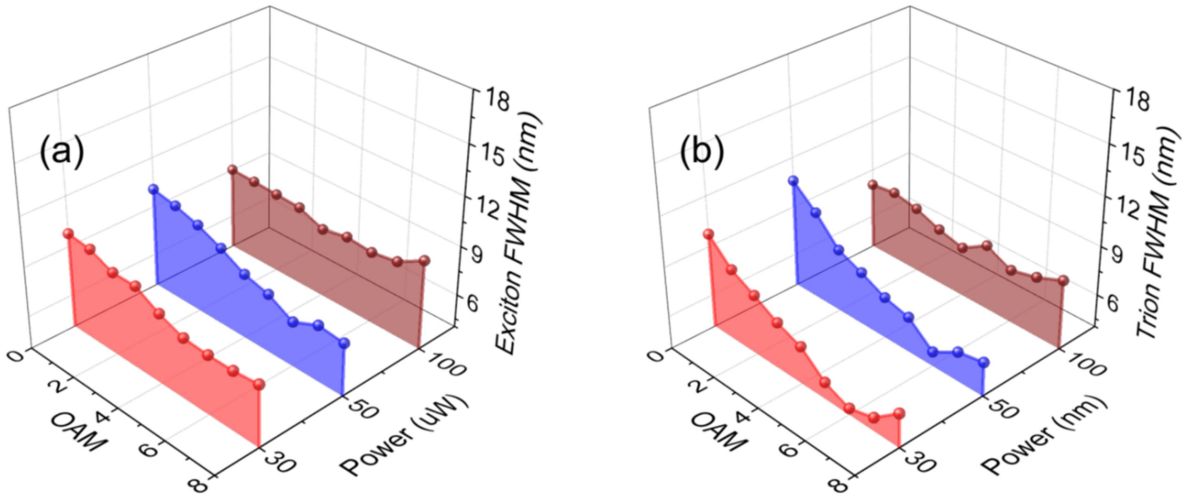

Figure S11. Linewidth analysis of deconvoluted PL spectra. FWHM of (a) excitons and (b) trions at 77 K as a function of OAM and laser power extracted from Figure S5. The exciton FWHM is nearly independent of either the OAM or the laser power. The trion FWHM exhibits a slight decrease with increasing OAM for the laser power at 30 μW and 50 μW.

Note 1. Calculation of the density of unbound electrons at the Fermi/defect level using the mass action law.

The mass action law for excitons and trions is defined as follows:

$$\frac{n_{Xo}n_{e-}}{n_{X-}} = K(T) = \frac{4m_{eff}K_BT}{\pi\hbar^2} exp\left(-\frac{E_{X-}^b}{K_BT}\right) \quad (1)$$

$$m_{eff} = \frac{m_{Xo}m_e^*}{m_{X-}}, \quad m_{Xo} = \frac{m_e^*m_h^*}{(m_e^*+m_h^*)}, m_{X-} = \frac{m_e^*(m_e^*+m_h^*)}{(2m_e^*+m_h^*)}.$$

Here,

$\frac{n_{X-}}{n_{X0}} \sim \frac{A_{trion}}{A_{exciton}} \sim 2.783$ (For 30 μW at ℓ = 0); $A_{exciton}\ and\ A_{trion}$ are the spectral areas of excitons and trions in the PL spectrums, respectively.

$E_{X-}^b = E_{Xo} - E_{X-} \sim 0.0238\ eV$ (For 30 μW at ℓ = 0); E_{Xo} and E_{X-} are the peak positions of excitons and trions in the PL spectrum, respectively.

$$m_e^* = 0.31\ m_e;\ m_h^* = 0.42\ m_e; m_e = 9.109 \times 10^{-31} Kg.$$

From equation (1), we find that

$$n_{e-} = 1.097 \times 10^{13} exp\left(-38.75E_{X-}^b\right) \times \left(\frac{A_{trion}}{A_{exciton}}\right).$$

Inserting all parameters given above for 30 μW laser power at the fundamental mode of light (ℓ = 0), we obtain

$$n_{e-} = 1.215 \times 10^{13} cm^{-2}$$